

Yb:YAG and Nd:YAG edge-pumped slab lasers

T. S. Rutherford, W. M. Tulloch,* S. Sinha, and R. L. Byer

Edward L. Ginzton Laboratory, Stanford University, Stanford, California 94305

Received February 7, 2001

Experimental demonstrations of two edge-pumped zigzag slab lasers are presented. The Nd:YAG slab laser generated 127 W of multimode output power with 300 W of pump power. Preliminary results with a Yb:YAG slab produced 46 W of output power with 315 W of pump power. The edge-pumped slab design permits symmetric conduction cooling and efficient pump absorption and accepts large-numerical-aperture pump sources. © 2001 Optical Society of America

OCIS codes: 140.3480, 140.3530, 140.5680, 140.3410, 140.3320.

Improvements in the brightness of laser-diode pump sources, both fiber-coupled and bare arrays, have provided the ability to push the limits of high-power solid-state laser design. Stress-induced birefringence, thermal lensing, and the stress-fracture limit make scaling of rod lasers to high average powers difficult when good beam quality is required. Zigzag slab geometry lasers have been scaled to high average power levels while maintaining good beam quality and polarization contrast.^{1–5} However, practical use of slab lasers has been limited by the low laser efficiency that is typically seen in side-pumped slab lasers and by the complexity of the pumping and cooling interface in the slab laser-head design. We have developed a zigzag slab laser design based on conduction cooling and a novel pumping geometry called edge pumping. The edge-pumping geometry decouples the cooling and optical pumping interfaces, simplifying the laser-head design. The advantages of this design include efficient pump absorption, acceptance of high-numerical-aperture pump sources, uniform conductive cooling, and scalability. This design is also compatible with quasi-three-level gain media.⁶ In this Letter we present the results of laser oscillation with Nd:YAG and Yb:YAG.

An ideal slab design requires that the slab be uniformly heated throughout its volume and uniformly cooled through the two total-internal-reflection (TIR) faces.⁷ Conventional designs have satisfied the requirement for uniform heating of the slab volume by specifying pumping of the slab through the TIR faces, a procedure that is known as face pumping.^{8,9} Using the same interface for pumping and cooling places significant engineering constraints on the slab laser design. Face-pumped designs typically require direct liquid cooling for uniform pumping and cooling of both faces. This requirement complicates the laser-head design and can lead to slab degradation or damage caused by contamination from the cooling fluid. Additionally, there is often a trade-off between thermal handling and pump absorption. Improved thermal handling requires reducing the slab thickness, but this reduces the pump absorption depth in a face-pumped geometry.

The edge-pumped slab represents a significant departure from conventional zigzag slab designs. Fig-

ure 1 shows a schematic of an edge-pumped slab. The slab is still uniformly cooled on the TIR faces; however, the pump power is incident from the non-TIR faces along the slab width, transverse to the thermal gradient and the direction of optical propagation. The design of the cooling interface no longer requires a material that is transparent to the pump radiation, providing the opportunity for conduction cooling. Also, because the absorption length is not in the cooling plane of the slab, one can reduce the slab thickness to improve the thermal handling of the slab without affecting the pump-power absorption.

The advantages of conduction cooling were recognized early in the development of slab lasers.¹⁰ Cooling uniformity, mechanical stability, protection of the TIR faces, and the separation of the slab-liquid interface are often cited as the benefits of conduction cooling. Experimental demonstrations of conduction cooling through a thin static layer of He gas in lamp-pumped Nd:Glass lasers confirmed these benefits.¹¹ More recently, conductive cooling of high-power thin disk lasers¹² and one-sided conduction cooling of slabs¹³ have been demonstrated. However, the asymmetries of these cooling schemes lead to thermal stresses in the crystals that limit the power-scaling potential. The symmetric cooling of the edge-pumped slab laser provides a design that can be scaled to high power levels.

We applied the edge-pumped slab design to Nd:YAG and Yb:YAG gain elements. Although they are

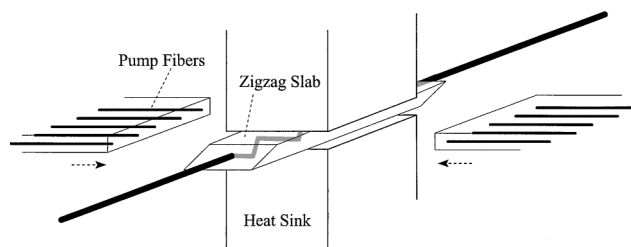


Fig. 1. Perspective view of the edge-pumped slab laser geometry. The conductively cooled slab is clamped in a water-cooled copper heat sink. Pumping by fiber-coupled laser diodes is illustrated, but other pump delivery methods could be used. For clarity the pump fibers are shown moved back from the laser head.

conceptually similar, the two lasers had some significant differences. The Yb:YAG slab was much smaller and utilized a composite crystal to ensure high-pump-power densities in the active region. Also, unlike the 808-nm laser diodes for pumping the Nd:YAG laser, the laser diodes for Yb:YAG did not require individual temperature control because of the comparatively broad absorption in Yb:YAG at 940 nm.

The details of the Nd:YAG laser are presented first: The 1% doped Nd:YAG slab measures 1.45 mm in thickness, 4.57 mm in width, and is 35.7 mm in length at the center line. The Brewster angle ends refract the beam onto a 16-bounce zigzag path. The TIR faces have a 2.5- μm coating of SiO_2 to protect the reflection. The edge faces are antireflection coated at the pump wavelength (808 nm). The slab is pumped by 30 fiber-coupled laser diodes, each of which has a maximum power of 10 W at the output of a 600- μm , 0.4-N.A. fiber.

At the full pump power the thermal focal length of the Nd:YAG slab is 470 mm in the zigzag plane and 420 mm in the nonzigzag plane. The average temperature of the slab at full power was measured interferometrically¹⁴ to be 42 °C with cooling water at 10 °C. Images of the fluorescence indicate relatively uniform pump absorption. The fluorescence intensity at the center of the slab is 80% of that at the slab edges.

The Nd:YAG slab was operated with three resonator configurations. The results are shown in Fig. 2. The multimode resonator consists of a 100-mm radius-of-curvature high reflector, a 100-mm focal-length lens, and a flat output coupler. The slab is placed between the high reflector and the lens, which are spaced 137 mm apart. The lens and the output coupler are separated by 24 mm. The mode waist in the slab is $\sim 130\ \mu\text{m}$, and, because the slab is the limiting aperture, many higher-order modes are excited in both axes. As the mode fills the entire aperture, the slope efficiency is not reduced by imperfect mode overlap ($\eta_B = 1$). This cavity resulted in a maximum output power of 127 W for 300 W of pump power with a 58% slope efficiency. The efficiency factors are estimated as follows: photon efficiency, $\eta_s = 808\ \text{nm}/1064\ \text{nm} = 76\%$; quantum efficiency, $\eta_q = 95\%$ output coupling efficiency, $\eta_c = 92\%$ (1% single-pass slab loss, 23.5% output coupling). From these estimates the pump absorption efficiency is derived to be 87%, which is consistent with the analysis in Ref. 6. The slight reduction in slope efficiency at the highest pump powers is due to residual depolarization losses near the slab edges.

The second resonator is designed with a larger mode size such that only the fundamental mode ($M_y^2 = 1.42$) can run in the thickness direction. Because of the 3:1 aspect ratio, the output is still multimode in the width direction. Because of slow degradation of the pump diodes after the resonator experiment, the maximum available power was reduced to 200 W. At this pump power, 55 W of output power was achieved, with a 39% slope efficiency.

TEM_{00} -mode output was achieved by use of intracavity cylindrical lenses to create a 3:1 elliptical mode to match the slab aspect ratio. The maximum power

achieved in this mode was 28 W for 175 W of pump power at a 22% slope efficiency. The M^2 at this power level was 1.47 in thickness and 1.50 in width.

An edge-pumped slab is also demonstrated, with Yb:YAG as the active medium. The slab is a diffusion bonded composite crystal of undoped YAG and 2% Yb:YAG. The undoped regions serve primarily to reduce the quasi-three-level reabsorption losses in the unpumped areas. The overall slab dimensions are 0.91 mm \times 7.1 mm \times 8.4 mm. As for the Nd:YAG slab, the ends are at Brewster's angle and the TIR faces have a SiO_2 coating. The doped region has the same 0.91-mm thickness as the entire slab but is 5.34 mm wide and 2.81 mm long. The crystal is held between two copper microchannel cooling blocks with indium foil to provide even thermal contact.

To suppress parasitic oscillations in the width-thickness plane,¹⁵ we polished one edge face at a 5° angle to the thickness direction and at a 2° angle to the length direction. This procedure was sufficient to completely eliminate parasitic oscillations up to the full pump power.

The slab was pumped by 10 laser diodes, each emitting from a 400- μm , 0.37-N.A. fiber. The laser was designed to use the rated power of 50 W per diode. Unfortunately, some diodes began to fail catastrophically near 30 W of power, so the total pump power was limited to ~ 300 W. Figure 3 shows the results achieved with a multimode resonator. The resonator was essentially the same as that used for the Nd:YAG multimode oscillator, except here a higher-reflectivity output coupler ($T = 9.1\%$) was used. Without any pump reflector at the slab edges, the slope efficiency was 24%. The addition of a gold reflector surrounding the pump fibers improved the slope efficiency to 28%. The inset shows the gain measured by a Yb:YAG microchip laser¹⁶ at 1030 nm. Transparency is achieved at 80 W of pump power. The sublinear character of the gain coefficient is a result of ground-state population depletion.

A breakdown of the efficiency terms gives the following results: The photon efficiency is $\eta_s = 91\%$,

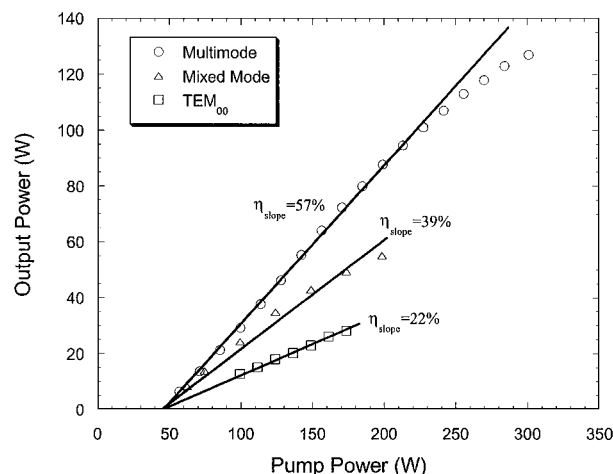


Fig. 2. Output power versus pump power for the Nd:YAG edge-pumped zigzag slab laser. The pump power was measured at the output of the fiber array.

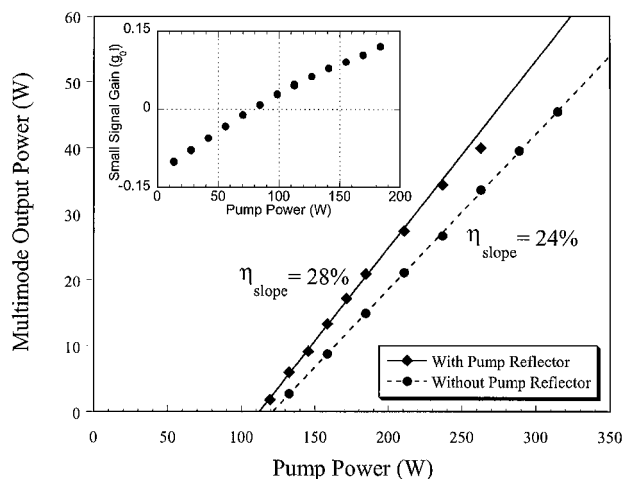


Fig. 3. Output power versus pump power for the Yb:YAG edge-pumped zigzag slab laser. The output power was limited only by the available pump power. Inset, single-pass small-signal gain as a function of pump power.

and the quantum efficiency η_q is assumed to be 100%. The output coupling efficiency is $\eta_c = 0.091/(0.033 + 0.091) = 73\%$. The transmission of the pump light through the uncoated slab edges is 92%. Because of errors in crystal fabrication (the doped region was not centered along the slab length), there was incomplete mode overlap in the thickness direction. M^2 in this direction was 2.3, which corresponds to a mode overlap efficiency of $\eta_B = 70\%$, given the cavity's fundamental mode size in the slab. From these efficiencies, the pump absorption is estimated to be 56% for no pump reflector and 65% with the pump reflector. These results compare well to the optimum value of $1 - \exp(-2 \times 0.534) = 66\%$ for a single pass of the pump light at the peak absorption wavelength. The small discrepancy is due to variations in the wavelengths of the pump diodes, which did not have individual temperature control.

Edge-pumped slab lasers have been demonstrated with Nd:YAG and Yb:YAG crystals. The Nd:YAG has a 58% multimode slope efficiency. In preliminary Yb:YAG experiments, 28% slope efficiency was observed. Improvements in crystal fabrication and pump diode performance should allow this slope efficiency to approach 60%. These results provide a starting point for power-scaling calculations that predict average powers of as much as 100 kW may be possible with Yb:YAG edge-pumped slabs.⁶

The authors thank T. Taira for providing the Yb:YAG microchip laser used in measuring the small-signal gain of the slab. This research was supported in part by National Science Foundation grant

PHY-9900793-002, by National Aeronautics and Space Administration grants NAG5-7709 and NAS1-00104, and by U.S. Air Force Office of Scientific Research grants F49620-99-1-0200 and F49620-99-1-0270. T. S. Rutherford's e-mail address is rutherf@stanford.edu.

*Present address, Positive Light, Los Gatos, California 95032.

References

1. R. J. Shine, Jr., A. J. Alfrey, and R. L. Byer, *Opt. Lett.* **20**, 459 (1995).
2. B. J. Comaskey, R. Beach, G. Albrecht, W. J. Benett, B. L. Frietas, C. Petty, D. VanLue, D. Mundinger, and R. W. Solarz, *IEEE J. Quantum Electron.* **28**, 992 (1992).
3. M. Sato, S. Naito, H. Machida, N. Iehisa, and N. Karube, in *Advanced Solid State Lasers*, M. M. Fejer, H. Injeyan, and U. Keller, eds., Vol. 26 of OSA Trends in Optics and Photonics (Optical Society of America, Washington, D.C., 1999), pp. 2–4.
4. J. G. Ho, R. J. St. Pierre, J. Morais, J. Poylio, W. Long, M. Weber, and M. M. Valley, in *Advanced Solid State Lasers*, H. Injeyan, U. Keller, and C. Marshall, eds., Vol. 34 of OSA Trends in Optics and Photonics (Optical Society of America, Washington, D.C., 2000), pp. 28–31.
5. G. D. Goodno, S. Palese, J. Harkenrider, and H. Injeyan, in *Advanced Solid State Lasers*, OSA Technical Digest (Optical Society of America, Washington, D.C., 2001), pp. 3–5.
6. T. S. Rutherford, W. M. Tulloch, E. K. Gustafson, and R. L. Byer, *IEEE J. Quantum Electron.* **36**, 205 (2000).
7. T. J. Kane, J. M. Eggleston, and R. L. Byer, *IEEE J. Quantum Electron.* **QE-21**, 1195 (1985).
8. J. M. Eggleston, T. J. Kane, K. Kuhn, J. Unterhahrer, and R. L. Byer, *IEEE J. Quantum Electron.* **QE-20**, 289 (1984).
9. D. Mudge, P. J. Veitch, J. Munch, D. Ottaway, and M. W. Hamilton, *IEEE J. Sel. Top. Quantum Electron.* **3**, 19 (1997).
10. J. P. Chernoch, "Laser cooling method and apparatus," U.S. patent 3,679,999 (July 25, 1972).
11. M. Reed, K. Kuhn, J. Unterhahrer, and R. L. Byer, *IEEE J. Quantum Electron.* **QE-21**, 412 (1985).
12. A. Giesen, H. Hugel, A. Voss, K. Wittig, U. Branch, and H. Opower, *Appl. Phys. B* **58**, 365 (1994).
13. A. D. Hays, G. Witt, N. Martin, D. DiBiase, and R. Burnham, *Proc. SPIE* **2380**, 88 (1995).
14. T. Y. Fan and J. L. Daneu, *Appl. Opt.* **37**, 1635 (1998).
15. T. S. Rutherford, W. M. Tulloch, E. K. Gustafson, and R. L. Byer, in *Advanced Solid State Lasers*, H. Injeyan, U. Keller, and C. Marshall, eds., Vol. 34 of OSA Trends in Optics and Photonics Series (Optical Society of America, Washington, D.C., 2000), pp. 16–20.
16. T. Taira, W. M. Tulloch, R. L. Byer, and T. Kobayashi, *Electron. Commun. Jpn. Part 2 Electron.* **79**, 64 (1996).